MANAS Journal of Engineering
ISSN 1694-7398 | e-ISSN 1694-7398

Volume 13, Issue 1, (2025) Pages 64-78
https://doi.org/10.51354/mjen.1699996

A Numerical Analysis of the Effect of Corrugated Surface Profile on Heat Transfer in Turbulent Flow Through a Rectangular Mini-Channel

Muhammet Kaan Yeşilyurt[1,2,*], Mansur Mustafaoğlu[1,2]

[1] Deparment of Mechanical Engineering, Faculty of Engineering, Atatürk University, Erzurum, Türkiye, kaan.yesilyurt@atauni.edu.tr ORCID: 0000-0002-7207-1743

[2] Deparment of Mechanical Engineering, Faculty of Engineering, Atatürk University, Erzurum, Türkiye, mansour@atauni.edu.tr ORCID: 0000-0003-2976-0196

ABSTRACT

Mini channels have the potential to provide high heat transfer efficiency in a variety of applications. However, due to their small size, higher pressure drop occurs. Therefore, a balance needs to be established between heat transfer improvement and pumping power requirements. In the present study the effect of corrugated surface profile on heat transfer and flow characteristics were numerically investigated under turbulent flow conditions in a rectangular cross-section mini-channel through Computational Fluid Dynamics (CFD) simulations using the ANSYS Fluent 2019 software. The study employed. The mini-channel had a total length of 26 mm, with the left and right side walls consisting of 3 mm straight sections at the inlet and outlet, and a 19 mm corrugated section in the middle while the top and bottom sides are straight end to end. Optimum values for heat transfer and pressure drop were investigated through CFD analyses by varying the profile of the corrugated section of the side walls between 0.5, 1 and 2 mm for air and water fluids. It was determined that the pressure drop for air varied between approximately 850-1250 Pa whereas for water it varied between 1300-1900 Pa. The Nusselt number increased by 3.27% for air, from 12.2 to 12.6, and for water, it increased by 2.17%, from 13.36 to 13.65. Results showed that the corrugated surface improved heat transfer by increasing turbulence and mixing with the flow, but also significantly increases the pressure drop.

ARTICLE INFO

Research article

Received: 15/05/2025
Accepted: 17/06/2025

Keywords:
Mini-Channel,
Heat Transfer,
Pressure Drop,
Corrugation

*Corresponding author

1. Introduction

In various systems, such as heat exchangers, nuclear reactors, and distillation units, mass and heat transfer occur along the walls of ducts where fluids flow. The fluid passage medium can be influenced by the cross-section of the channel as the volumetric flow passes over it, affecting the transfer processes. The utilization of smaller-sized channels, such as mini- and micro-channels, presents a significant opportunity to enhance heat transfer efficiency in various applications [1]. Mini-channels are channels that are larger than micro-channels, but with a hydraulic diameter typically between 0.1 mm and 6mm. They offer a balance between the high efficiency of micro-channels and the easier manufacturing of larger channels. Mini-channels play a crucial role in enhancing heat transfer efficiency in various applications. While smaller channels offer improved heat transfer efficiency, they also result in a higher pressure drop per unit length. It is therefore necessary to keep a balance between heat transfer enhancement and pumping power requirements [2].

In automotive applications, as a result of miniaturization, the size of radiators and evaporators has become crucial to achieving an optimal balance between the pumping power requirements, heat transfer efficiency, and cleaning of the entire system. Specifically, the dimensions of these components are often reduced to the millimeter scale to maximize cooling performance while minimizing energy consumption. Similarly, in building air conditioning applications, advancements in thermal management systems now allow for the integration of electronic and microelectronic cooling solutions with centralized HVAC systems. Such integrations have been particularly important for the equipments where a stable thermal environment is critical for operational efficiency, such as server rooms [3]. These developments and associated integrations increase the demand for compact and efficient cooling technologies across various applications.

Increased power density along with minituarization of electronic devices brought on the need for an effective thermal management in electronic components as high temperatures have great negative impact on performance and life of electronic devices [4]. Therefore, compact cooling systems, especially those made using micro and mini channels, have become an important research topic since they offer higher heat transfer efficiency compared to traditional air-cooled methods [5].

Mini channels typically have hydraulic diameters ranging from 1 to 10 mm and provide effective heat transfer thanks to their high surface-to-volume ratio [6]. In this study, a mini channel array with straight and reversely arranged semicircular bends was investigated as a heat sink for cooling electronic components. The reason for choosing this particular configuration is that the vortices formed with the change of direction of the flow increase the heat transfer coefficient and provide a more homogeneous temperature distribution.

Many studies have been conducted in the literature on the heat transfer of mini channels with similar structures. For example, Kandlikarand Grande [7], in their studies examining the effect of mini channel geometry on heat transfer, showed that the flow regime in micro-scale channels exhibits different characteristics compared to traditional channels. In addition, Leeand Garimella [8] presented a detailed analysis of the flow and heat transfer characteristics in cooling systems using mini channel arrays.

Harley et al. [9] measured the friction factor (C_f) in multi-sided and square-section micro-channels. Experimentally, they found that C_f was 49 for square channels and 512 for multilateral channels. Pengand Peterson [10] experimentally revealed that the transition to turbulent flow starts in the range of Reynolds 200–700, and the full turbulent transition is reached at Reynolds 400–1500. They also observed that Reynolds decreases as the microchannel becomes smaller. Pengand Wang [11] concluded that this feature is due to the thermo-physical properties of the fluid due to the high heat flux in the micro-channels.

Shahand London [12] demonstrated that equilateral triangular cross-section micro-channels can lead to a 17% reduction in the friction factor for developed laminar flow at constant heat flux, despite a 27% penalty in the Nusselt number. This finding highlights the trade-off between friction factor reduction and Nusselt number in micro-channels with specific geometries. Additionally, Steinkeand Kandlikar [13] discussed the ongoing research on the validity of friction factor theory for microchannel flows based on conventional-sized passages. This suggests that there is still active exploration and debate regarding the applicability of traditional friction factor theories to microscale flows. Moreover, research by Wang et al. [14] indicated that adding ribs to micro-channels can enhance heat transfer performance but inevitably increases the friction factor. The study found that the friction factor increased significantly for micro-channels with rectangular, triangular, and semicircular ribbed configurations compared to smooth micro-channels. This emphasizes the impact of channel modifications on friction factor values.

Comparison of numerical calculations of flow in trapezoidal channels for flows with Reynolds numbers below 600 showed a good match between numerical and experimental results, although inflow effects can be seen in very short channels [15].

Heat transfer research on mini-channels has received significant interest due to the potential for enhanced heat transfer efficiency in compact systems. Mini-channels improve heat transfer in two primary ways: by increasing the heat transfer coefficient through their small dimensions and reducing resistance on airflow due to their flat orientation [16]. Research has explored various aspects of mini-channel heat transfer, including the impact of different geometrical designs on heat transfer rates, with a particular emphasis on the use of different fluids to improve heat transfer efficiency [17]. Additionally, investigations into the effects of roughness on laminar heat transfer in additive manufactured mini-channels have shown that roughness can indeed enhance heat transfer performance [18].

Alterations to channel walls, such as the introduction of ribs or wavy patterns, can significantly influence heat transfer processes. Research has shown that the integration of ribbed surfaces in heat exchangers has been widely adopted to enhance convective heat transfer and overall thermal efficiency [19]. The addition of ribs can also lead to a substantial increase in the friction factor [20]. Furthermore, ongoing research explores the validity of traditional friction factor theories for mini- and micro-channel flows, highlighting the intricate relationship between channel geometry, modifications, and their impact on friction factors and heat transfer performance in diverse fluid systems. On the other hand, the incorporation of porous inserts in channels can significantly enhance convective heat transfer while moderately increasing flow resistance [21]. The application of nanofluids and unique channel geometries, such as triangular wavy channels, under pulsating flow conditions has been investigated to understand their impact on heat transfer and pressure drop characteristics [22].

Alhamid et al. [23] conducted a study on the effect of turbulators on thermal flow and heat performance in a 3D pipe, exploring different concavity diameters with corrugation and twisted tape configurations. This research aimed to improve heat transfer efficiency through innovative design modifications. Similarly, Al-Obaidi et al. [24] studied flow field and heat transfer enhancement using a combination of corrugated tubes with a twisted tape within a 3D circular tube based on different dimple configurations.

Mezaache et al. [25] investigated mixed convection and entropy production of nanofluid flow in a corrugated channel using a two-phase mixture model, exploring corrugation profiles with trapezoidal, sinusoidal, and triangular shapes. Additionally, Haj Maideenand Somu [26] analyzed the design and performance of a double-pipe heat exchanger with new arrangements of corrugated tubes using honeycomb arrangements, focusing on convective heat transfer and friction factor of Al_2O_3-water nanofluid in helically corrugated tubes.

Choudharyand Ray [27] conducted a numerical study on combined convection heat transfer flow in a porous corrugated enclosure, investigating the influence of the Grashof number on heat transfer efficiency. Sruthi et al. [28] performed a comparative analysis of the corrugation effect on the thermohydraulic performance of double-pipe heat exchangers, focusing on the effectiveness of helically corrugated tubes in enhancing convective heat transfer.

Songand Wang [29] have emphasized the importance of secondary flows to enhance heat transfer performance while minimizing pumping power requirements and thermal resistance. Additionally, specialized channel designs, such as corrugated channels, has been shown to significantly enhance heat transfer.

Microelectronic equipment with various applications, such as personal computers, servers, general diodes, etc., has been proposed to increase the intensity of the transmitted heat flow to higher values, thus increasing the once very large and unattainable figure of 200 watts per square centimeter of transmitted heat, has now become a normal or even small amount. As a matter of fact, heat transfer rate is over 600 watts per square centimeter today. In addition, the temperature difference required to carry out the heat transfer process is also decreasing by a few degrees Celsius. These high amounts of heat transfer require that the dimensions of the micro-channels be greatly reduced so that they can be well matched to the components of the cooling system and thus improve the movement of the fluid from the heat source [30].

In this research, therefore, a 26-mm-long mini-channel was designed with a 3 mm straight upstream part, a 20-mm central part with corrugated side walls, and another 3mm straight downstream part. These channels are capable of being coupled with each other, by being putting together one straight and one reversed, to form wider arrays of mini-channels to function as a heat sink as shown in Figure 1.

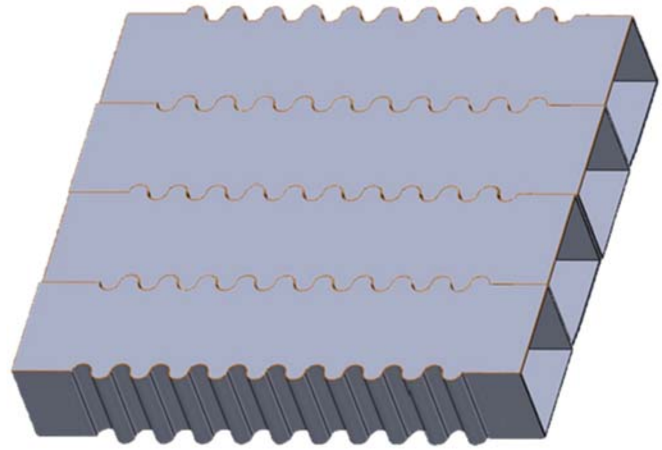

Figure 1. *Heat sink consisting of array or mini-channels*

In this respect, the effect of a channel geometry on the flow characteristics and cooling performance was numerically investigated for certain input parameters and boundary conditions. While previous research has explored the influence of various geometric modifications on thermal performance, the channel configuration is unique in terms of wall structure, dimensions, arrangement, and profile. Computational Fluid Dynamics (CFD) simulations were conducted using ANSYS Fluent software to evaluate the impact of these modifications on pressure drop, Nusselt number, and velocity distributions for both air and water as working fluids. The findings contribute to a deeper understanding of how surface profiling can enhance heat transfer efficiency while minimizing energy losses in practical engineering applications.

2. Materials and Methods

2.1. Governing Equations

The integral form of continuity laws is valuable for analyzing the overall behavior of flow fields, while a deeper understanding of flow field specifics necessitates the use of the differential form of fluid motion equations. The governing equations for heat transfer in differential form involve conservation of mass, momentum and energy [31; 32]. First, the assumptions governing the problem are examined:

Turbulent flow.

- The physical properties of the fluids are constant.
- The fluid is incompressible, Newtonian and viscous.
- No-slipwall condition was applied to the computational domain to ensure that the velocity at the solid-fluid interface is zero, in accordance with the standard assumptions of viscous flow [33].
- Constant heat flux to the bottom wall without corrugation.
- No heat loss from external surfaces

Considering the flow in mini-channels of rectangular cross-section, similar to the flow between two parallel planes, the equations governing the flow are simplified to the following forms.

The continuity, momentum and energy equations governing the problem are as follows [34]:

$$\frac{\partial \rho}{\partial t}+\frac{\partial(\rho u_j)}{\partial x_j}=0 \tag{1}$$

$$\frac{\partial(\rho u_i)}{\partial t}+\frac{\partial(\rho u_j u_i)}{\partial x_j}=-\frac{\partial P}{\partial x_i}+\frac{\partial \tau_{ij}}{\partial x_j}+S_{ui}$$

which can be expanded as:

$$\frac{\partial}{\partial x_j}(\rho u_i u_j)=-\frac{\partial p}{\partial x_i}+\frac{\partial}{\partial x_j}\left[\mu\left(\frac{\partial u_i}{\partial x_j}+\frac{\partial u_j}{\partial x_i}-\frac{2}{3}\delta_{ij}\frac{\partial u_i}{\partial x_j}\right)\right]+\frac{\partial}{\partial x_j}\left(-\rho\overline{u'_i u'_j}\right) \tag{2}$$

The energy equation is:

$$\frac{\partial}{\partial x_i}(\rho u_i c_p T)=\frac{\partial}{\partial x_j}\left[\left(k+\frac{c_p\mu_t}{Pr_t}\right)\frac{\partial T}{\partial x_j}+u_i\left(\mu_{eff}\left(\frac{\partial u_j}{\partial x_i}+\frac{\partial u_i}{\partial x_j}\right)-\frac{2}{3}\mu_{eff}\frac{\partial u_i}{\partial x_j}\delta_{ij}\right)_{eff}\right] \tag{3}$$

This model is well suited for confined flows. It is also suitable for deceleration and sudden separation flows with pressure gradients. The concept of turbulent viscosity is also used in the solution.

$$\frac{\rho\partial k}{\partial t}+\rho u_j k_j=\left(\mu+\frac{\mu_t}{\sigma_t}k_j\right)+G+B-\rho\omega k \tag{4}$$

$$\frac{\rho\partial \omega}{\partial t}+\rho u_j \omega_j=\left(\mu+\frac{\mu_t}{\sigma_t}\omega_j\right)+\frac{c_1\omega}{k}G+\frac{c_1\omega}{k}(1-C_3)B-C_2\rho\omega^2 \tag{5}$$

2.2. Geometric Model and Boundary Conditions

The geometric model consists of a rectangular mini-channel with corrugated side walls. The geometric parameters of the model used in this study is given in Table 1.

Table 1. Design parameters

Parameter	Notion	Value
Height of the channel	H	5mm
Width of the channel	W	6mm
Corrugation radius	r	0.5mm
Corrugation pitch	λ	1 mm
Upstream section	U	3mm
Corrugated Central section	C	20mm
Downstream section	D	3mm
Pitch-to-width ratio	λ/W	0.200
Pitch-to-length ratio	λ/H	0.167

The drawing of the duct geometry to be analyzed was drawn with the Solidworks program and then these geometries were exported to the ANSYS Workbench program and the mesh structure was created in this program. Since the duct geometry examined in this study is symmetrical, the channel geometries were drawn square and the mesh structure was created accordingly. Figure 3 shows the mesh structure created for the analysis of the channel geometry. A symmetry boundary condition was applied at the mid-plane of the mini-channel to reduce computational cost and ensure an accurate representation of flow characteristics. The symmetric plane divides the geometry into two equal halves along the longitudinal axis, assuming identical flow behavior on both sides of the plane [35].

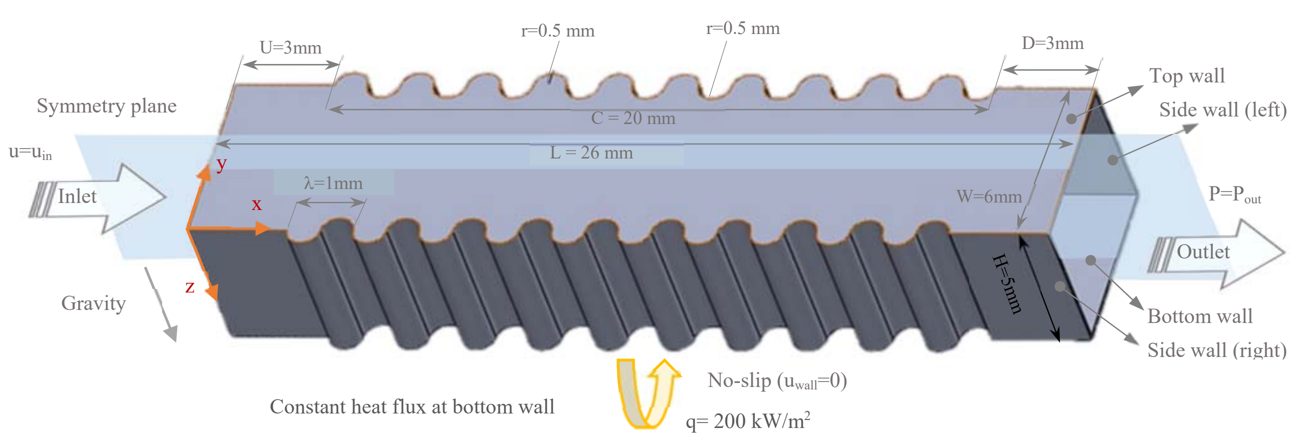

Figure 2. *Channel geometry and boundary conditions*

Figure 2 illustrates the computational domain of the mini-channel, including all relevant boundary conditions and dimensions. The total length of the mini-channel is 26 mm, with a 3 mm straight section at the inlet, a 20 mm corrugated section in the middle, and another 3 mm straight section at the outlet. The corrugated wall introduces periodic disturbances to the flow, enhancing turbulence and heat transfer.

The boundary conditions for the computational domain were adopted as follows:

Inlet boundary conditions	Wall boundary conditions	Outlet boundary conditions
$u = u_{in}$	u = 0	$\frac{\partial \emptyset}{\partial n} = 0,$ $\emptyset = u, v, p, k, \omega$
v = w = 0	v = 0	$\frac{\partial u}{\partial x} = \frac{\partial v}{\partial x} = \frac{\partial w}{\partial x} = 0$
$T_{in} = 293.15k$	$q = q_{wall}$	$\frac{\partial T_f}{\partial x} = 0$
$k = k_{in}$		$\frac{\partial k}{\partial x} = 0$
$\omega = \omega_{in}$		$\frac{\partial \omega}{\partial x} = 0$

In order to reduce the computational cost and also maintain accuracy, a symmetry boundary condition is applied along the mid-plane of the channel, effectively. The walls are treated as no-slip boundaries, and a constant heat flux of 200 kW/m^2 is imposed on the bottom wall to evaluate heat transfer performance.

2.3. Meshing and Numerical Solution

In this study, tetrahedral mesh elements were used during the creation of the examined duct geometry. The meshed model consisted of about 8 million elements. In order to calculate the distance of the first mesh element from the wall, the value of (y^+) was initially chosen as 5. After finding the distance of the first mesh element from the wall, twenty layers were drawn in the regions close to the wall with a growth rate of 1.2. Thus, in order to calculate and examine the regions close to the wall more precisely, the mesh structure was densified in the regions close to the wall.

a

b

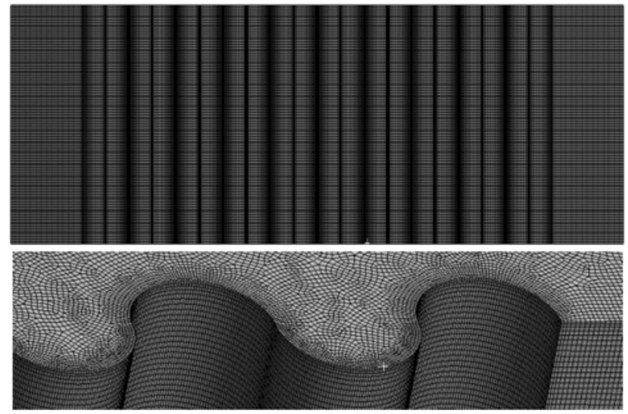

Figure 3. *(a) Meshed model in top view of the right side-wall (b) Close-up view of near wall zone with mesh refinement*

As seen in Figure 4, a grid independence test was conducted to verify that the results were not sensitive to mesh refinement. Five different mesh sizes (coarse, medium, fine, finer, and extra fine) were tested, and the variation in the Nusselt number and maximum temperature was monitored. The deviation was found to be within 1.2%, confirming the adequacy of the selected grid resolution.

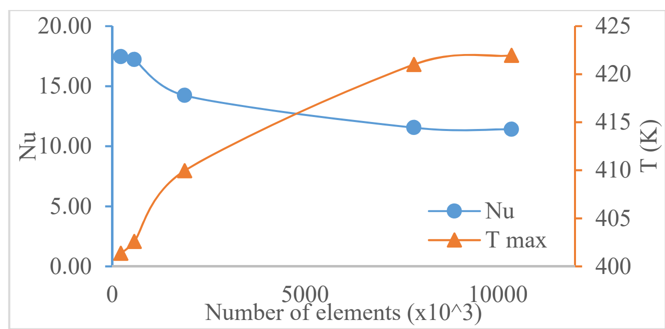

Figure 4. *Grid independence based on variation of Nu and T at different meshes at Re 2300*

The flow near the wall is analyzed according to the general characteristics of our geometry. Since the Reynolds range is small and the flow is limited, the k-ω and k-ε methods give the best response.

The flow structure in the created duct geometry was analyzed using numerical calculation techniques. No data were obtained with any experimental setup. Computational fluid dynamics (CFD) simulations and data were obtained using the ANSYS FLUENT CFD software. The geometries analyzed using the ANSYS FLUENT program were first drawn with the Solidworks CAD software, and then the mesh structures for these geometries were created in the Mesh Structure Creation module of the ANSYS Workbench in accordance with ANSYS FLUENT.

Turbulent fluid motion represents a dynamic flow state characterized by random variations in flow quantities across both space and time, such that a statistically significant mean can hardly be distinguished [36]. Notably, the k-ω turbulence models, developed primarily for aerospace applications involving intricate geometries and phenomena, offer a more straightforward foundation compared to the k-ε turbulence model pioneered by Wilcox. These models present a key advantage in that they allow for the resolution of equations down to the viscous substrate, a capability not always achievable with k-Ɛ models. Among the widely utilized k-ω turbulence models are the standard k–ω turbulence model and the SST k-ω turbulence model, each offering unique insights into turbulent flow behavior. k - ω models are said to be based on much simpler foundations than the k-ε turbulence model [37]. The k-ω turbulence models were originally developed for aerospace applications with very complex geometries and phenomena. An important advantage of k-ω turbulence models over k-ε turbulence models is that the equations can be solved down to the viscous sub layer [38; 39]. The most widely used k-ω turbulence models are the standard k–ω turbulence model and the k-ω SST turbulence model.

The standard k-ω turbulence model incorporates the effects of low Reynolds number and compressibility effects into the calculations. The standard k-ω turbulence model is an empirical model based on the transport equations related to the turbulent kinetic energy (k) and the specific energy dissipation (ω). As the k-ω turbulence model has been evolving over the years, production terms have been added to the transport equations for k and ω that improve the prediction of free shear flows [40].

Due to its proven ability to accurately predict flows involving adverse pressure gradients and flow separation, which are likely to occur in corrugated or duct-like geometries, the k–ω SST model offers superior near-wall treatment by blending the k–ω model near walls with the k–ε model in the free stream, thus providing improved accuracy for wall-bounded turbulent flows. This makes it particularly suitable for the present study where capturing wall effects and pressure-induced separations is critical. The model has also been widely validated in similar studies involving duct flows and heat transfer enhancement with surface irregularities.

Transport equation for turbulence kinetic energy (k);

$$\frac{\partial(\rho k)}{\partial t}+\frac{\partial(\rho k u_i)}{\partial x_i}=\frac{\partial}{\partial x_i}\left[\Gamma_k\frac{\partial k}{\partial x_j}\right]+P_k-Y_k-S_k \tag{6}$$

Transport equation for specific energy dissipation (ω):

$$\frac{\partial(\rho\omega)}{\partial t}+\frac{\partial(\rho\omega u_i)}{\partial x_i}=\frac{\partial}{\partial x_i}\left[\Gamma_\omega\frac{\partial k}{\partial x_j}\right]+P_\omega-Y_\omega-S_\omega \tag{7}$$

In Equations (5) and (6), P_k is the production of turbulence kinetic energy (k), P_ω is the production of specific energy dissipation (ω), Γ_k and Γ_ω are the effective propagation power terms of turbulence energy (k) and specific energy dissipation (ω), respectively. The terms Y_k and Y_ω are the turbulence-induced dissipation of the turbulence kinetic energy (k) and the specific energy (ω), respectively.

In the study a steady-state turbulent flow condition was considered through the mini-channel, time-dependent terms were not included in the final numerical formulation. The solution was obtained using the SIMPLE algorithm for pressure-velocity coupling, and second-order upwind discretization was applied to convective terms to enhance accuracy.

Therefore, the k and ω equations can be re-written for the steady-state solution as follows:

$$\frac{\partial(\rho k u_i)}{\partial x_i}=\frac{\partial}{\partial x_i}\left[\Gamma_k\frac{\partial k}{\partial x_j}\right]+P_k-Y_k-S_k \tag{8}$$

$$\frac{\partial(\rho\omega)}{\partial t}+\frac{\partial(\rho\omega u_i)}{\partial x_i}=\frac{\partial}{\partial x_i}\left[\Gamma_\omega\frac{\partial k}{\partial x_j}\right]+P_\omega-Y_\omega-S_\omega \tag{9}$$

The convergence criteria were set to ensure numerical stability and solution accuracy. The residual values for continuity, momentum, and energy equations were monitored throughout the iterations, with a convergence threshold of 10^{-6} for the energy equation and 10^{-4} for other governing equations. The solution was considered converged when the residuals fell below these limits and when the temperature and velocity fields no longer exhibited significant variations between consecutive iterations.

The representation of the results of solution as well as the flow characteristics and heat transfer, some parameters and variables are needed. For a comprehensive analysis of the thermal and hydrodynamic performance of the mini-channel independent of geometric and operating conditions, key dimensionless parameters are handy.

The Reynolds number is a fundamental parameter that determines the flow regime within the mini-channel. It is defined as [41]:

$$Re=\frac{\rho U D_h}{\mu} \tag{10}$$

For the present study, the entrance velocity and fluid properties define the Reynolds number, which determines whether the flow is laminar ($Re<2300$), transitional ($2300\leq Re\leq 4000$), or turbulent ($Re>4000$).

Since mini-channels often operate near transitional conditions, special care must be taken in selecting appropriate heat transfer correlations.

The Nusselt number quantifies the convective heat transfer enhancement relative to conduction across the fluid. It is given by [42]:

$$Nu = \frac{hD_h}{k} \tag{11}$$

where h is the convective heat transfer coefficient, k is the thermal conductivity, and D_h is the hydraulic diameter calculated by [43]:

$$D_h = 4\frac{A}{P} = \frac{2WH}{W+H} \tag{12}$$

A higher Nu value indicates more efficient convective heat transfer. Turbulent flow conditions require empirical correlations such as Gnielinski's [44] or Petukhov's [45].

For hydrodynamically and thermally developing flow in a duct or channel, Shahand London [12] proposed a correlation for the Nusselt number:

$$Nu = 3.66 + \frac{0.0668 \cdot (D/L) \cdot Re \cdot Pr}{1 + 0.04 \cdot [(D/L) \cdot Re \cdot Pr]^{2/3}} \tag{13}$$

Where Prandtl number is [34]:

$$\Pr = \frac{\mu c_p}{\lambda} \tag{14}$$

Since the mini-channel modeled in this study has micro-scale features, modified correlations are better for accounting for entrance effects, wall roughness, and scale-dependent thermal effects. Another approach is to modify the Gnielinski correlation by interpolating between the laminar and turbulent regimes:

$$Nu = \left(\frac{Nu_{\text{laminar}} + Nu_{\text{turbulent}}}{2}\right) \times \left(1 + \left(\frac{Re - 2300}{4000 - 2300}\right)^2\right) \tag{15}$$

In mini-channels, Nu also depends on surface roughness and flow acceleration effects. Until Coulomb's experiments in 1800, the effect of surface roughness on frictional resistance was not known. Later, Prandtl's student Nikuradse simulated roughness by gluing uniform grains of sand onto walls of pipes, measured pressure drops and flow rates in these pipes, and examined the variation of the coefficient of friction with Reynolds number. According to Nikoradze's results, it can be concluded that flows in the approximate range (Y^+) between 12 and 250 have a strong relationship with the geometry of the channel and the best place to investigate the geometry is in this range. As a result of his investigations, he found that the coefficient of friction is not affected in laminar flow, but in turbulent flow, friction increases with the relative roughness *ε/d* after a certain initial point and can be calculated as follows [46]:

$$\frac{1}{f^{0.5}} = -2log\left[\frac{\varepsilon/d}{3.7} + \frac{2.51}{Re\, f^{0.5}}\right] \tag{16}$$

The Fanning friction factor, which is used in heat transfer and CFD studies, characterizes the pressure loss due to viscous effects and is defined as [47; 48]:

$$f = \frac{\Delta P D_h}{2\rho U^2 L} \tag{17}$$

For laminar flow, the theoretical friction factor for a smooth duct is:

$$f = 16/Re \tag{18}$$

In turbulent conditions, however, empirical relations such as the Blasius equation apply.

Considering the relative roughness coefficient *ε/d* and Reynolds number, the effect of surface roughness is not a matter of discussion in the present study. Nonetheless, the corrugation profile on the sidewalls of the mini-channel act as surface roughness, and can cause turbulent flow to occur by strengthening instability in the flow.

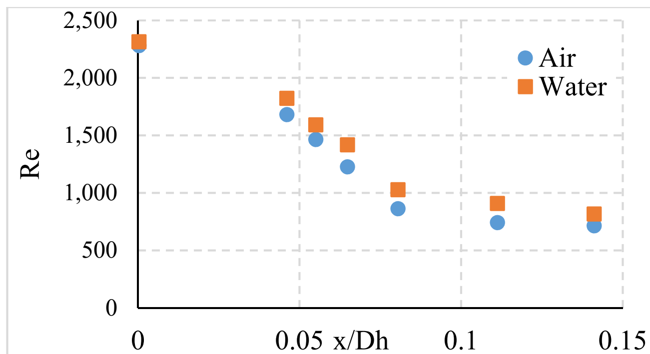

Figure 5. *Effective roughness in the channel*

Figure 5 shows critical Reynolds diagram against normalized channel length. With the help of different results obtained from experimental solutions, it is seen that the more the roughness in the channels, the less Reynolds reaches the turbulent flow. Besides, mini-channels exhibit entrance effects and possible micro-scale flow deviations that also induce turbulence in smaller Reynolds numbers.

As seen in Figure 5, corrugated surfaces can lower the critical Re significantly from about 2300 to some 700 depending on the amplitude, wavelength and shape of the corrugation as well as the type of the fluid and flow geometry.

A validation of numerical results is often necessary due to these mentioned peculiarities of mini-channels.

The pressure drop for the flow in the corrugated mini-channel is:

$$\Delta p = P_{in} - P_{out} = f\,\frac{(x_e - x_s)\rho {u_{in}}^2}{2D_h} \tag{19}$$

To assess the combined impact of heat transfer enhancement and pressure drop, the thermal performance factor is used [41; 43]:

$$\eta = \frac{(Nu/Nu_0)}{(f/f_0)^{1/3}} \tag{20}$$

where Nu0, and f0 are the baseline Nusselt number and friction factor for a conventional smooth channel. Thermal performance factor accounts for heat transfer enhancement relative to the increase in pressure drop through comparison across studies by normalizing against a baseline case, typically a smooth channel. This metric is best for comparing channels with different enhancement techniques but similar Reynolds numbers. A value of $\eta > 1$ indicates that the proposed mini-channel geometry provides an overall thermal improvement.

As stricter version of η, Performance Evaluation Criterion (PEC), which penalizes pressure drop more than η, is also used when comparing energy-efficient cooling solutions across different studies [49; 50]:

$$PEC = \frac{(Nu/Nu_0)}{(f/f_0)} \tag{21}$$

Another metric is Bejan number (Be) which evaluates the heat transfer enhancement against frictional losses. Greater Be indicates greater entropy generation due to friction and hence less efficiency. It is mostly preferred in analyzing heat transfer irreversibility in micro- or mini-channels and is best for comparing cooling strategies in thermodynamic optimization

$$Be = \frac{f}{Re \cdot Pr} \tag{22}$$

For a more flow-sensitive way of evaluation that accounts for both convective heat transfer and pressure drop, Modified Thermal-Hydraulic Factor (Θ) is often preferred to compare studies with different flow conditions or cases where Re varies significantly:

$$\Theta = \frac{Nu}{\sqrt{fRe}} \tag{23}$$

For small-sized thermal systems such as compact heat exchangers, Colburn Factor-to-Friction Factor Ratio (j/f) is used to evaluate heat transfer efficiency per unit pressure drop [34; 51]:

$$\frac{j}{f} = \frac{Nu}{RePr^{1/3}f} \tag{24}$$

3. Results and discussion

This study investigates how turbulence intensity and turbulence length scale affect heat transfer and flow characteristics for different geometries and different flow types using computational fluid mechanics. In many real flows, long and flat surfaces are encountered. Examples of situations where the boundary layer is formed on long and flat surfaces are flow over a ship hull, flow over a submarine hull, flow over aircraft wings, atmospheric flow over flat terrain. The flow characteristics over long and flat surfaces in engineering problems are similar to the flow over a flat plate. Therefore, understanding the flow on a flat plate is important for understanding the flow characteristics on long and flat surfaces in engineering problems.

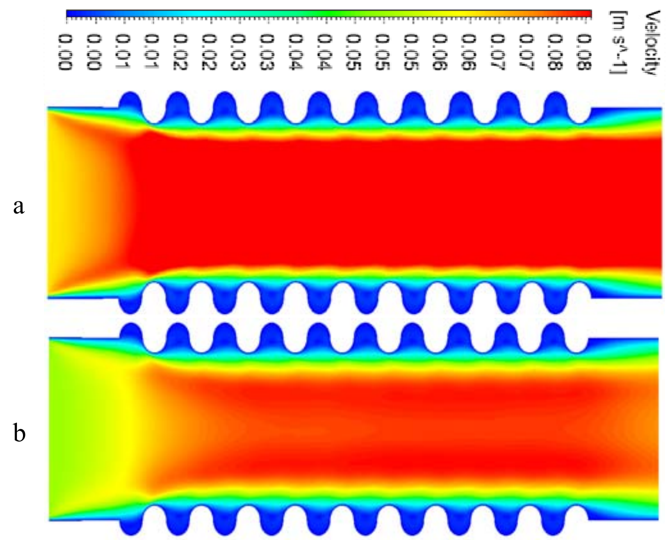

Figure 6. *Turbulent flow velocity profile in the channel at Re 2300 a) air b) water*

The standard k-ε, k-ω, RNG k-ε and SST models are compared among themselves and it can be concluded that the k-ω turbulence model gives better results than the other models, although the RNG k-ε model shows close performance. The velocity profile obtained from the graph for Reynolds 2300 and lambda 1000 micrometer range can be seen as follows. The longitudinal curvature in the velocity contours through the channel can also be seen below.

When the CFD velocity profiles for turbulent flow through the channel, given in Figure 6, are compared for air and water; it is clearly visible that the velocity profile for air shows a high-velocity core region (in red) concentrated in the longitudinal center part of the channel and that the velocity gradually decreases towards the walls, with blue regions indicating low-velocity zones at the pits (valleys) and relatively-higher low-velocity zones at the hills (crests). Flow is relatively uniform in the central region but shows deceleration near the corrugated surfaces, which suggests that the presence of corrugation creates higher resistance to the flow.

The fluid temperature distribution is shown as shown in Figure 7.

a
b

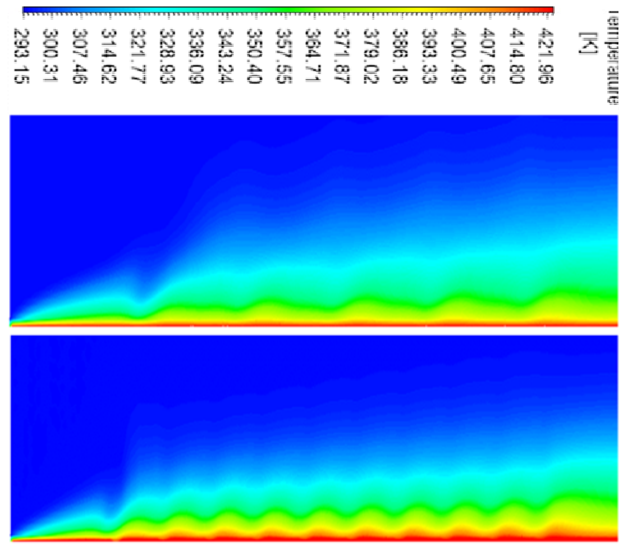

Figure 7. *Fluid temperature distribution through the channel at Re 2300 a) air b) water*

Comparing air and water, the transition of the profile from high- to low-velocity is more gradual for water than air and the deceleration near the walls is less steep than that of air. It is also notable that the effects at the entrance and exit are less pronounced for water and it could maintain a relatively-stable flow profile despite the corrugated surfaces, which indicates that water has a higher momentum due to its greater density and therefore the effect of corrugation on the flow profile is less. Likewise, air is more susceptible to flow disturbances and exhibits sharper gradients due to its lighter density and viscosity as manifested by sharper velocity gradient near the walls.

As seen in Figure 7, the temperature distribution for air shows a high-temperature region near the corrugated wall (in red) and a gradual transition to lower temperatures towards the centerline (in blue). The temperature gradient is steeper in air due to having lower thermal conductivity, lower specific heat capacity, and lower density. Air heats up more rapidly than water and exhibits a steeper temperature gradient which implies rapid cooling of the air as it moves through the channel. The high-temperature zone in water is more extensive and the temperature gradient is gentler due to its higher specific heat capacity, which suggests that water absorbs and distributes heat more uniformly and therefore maintains a higher temperature over a larger area. These findings clearly show the critical importance of fluid properties in determining thermal performance in corrugated channels.

a
b

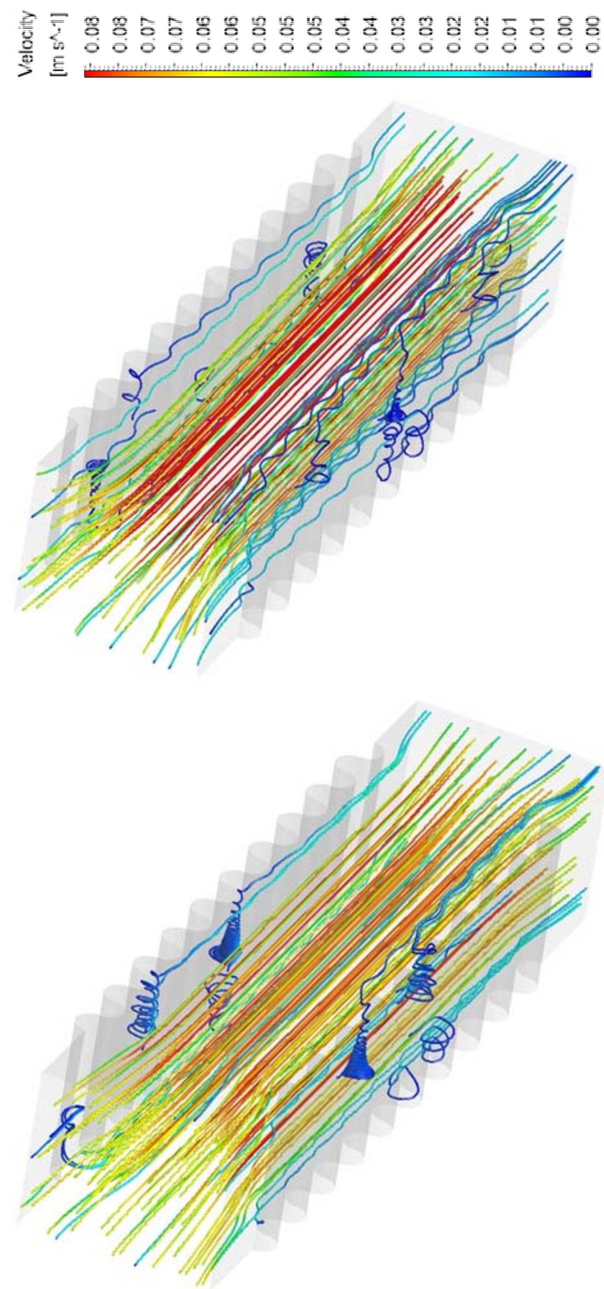

Figure 8. *Streamlines through the channel at Re 2300 a) air and b) water*

The streamlines of flow through the channel, shown in Figure 8, is also important to evaluate the distinct flow behaviors for air and water. With streamlines maintaining a relatively straight path, both fluids exhibit a high-velocity, undisturbed core region (red and yellow) through the central part of the channel. However, near the corrugated walls, both air and water show significant distortion of streamlines and the presence of secondary flow zones with recirculation. These recirculation zones, in blue (lower velocity), indicate areas of turbulence and mixing induced by the interaction with the corrugated surfaces.

For air flow, the high-velocity core remains largely undisturbed, ensuring efficient flow through the channel's center. However, the interaction with the walls generates vortices and turbulence, which could enhance mixing and heat transfer efficiency but also increase flow resistance. Water flow demonstrates similar characteristics, with a stable high-velocity core and pronounced recirculation zones near the walls. While secondary flows occurred in both air and water, stronger and more complex secondary flow patterns occurred in water due to its higher viscosity and density. While this might seem counterintuitive as air was mentioned above as more susceptible to flow disturbances, higher density leads to stronger inertial forces that contribute to the development of secondary flows and higher viscosity promote secondary flows due to increased shear stresses at the tube walls.

The most important comparison and validation parameter for ducts is the pressure drop. The Reynolds number is 2300 and the results of the pressure drop obtained from ANSYS Fluent are shown as follows

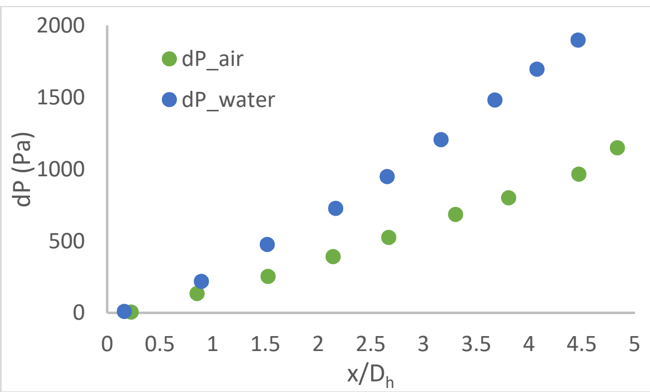

Figure 9. *Variation of pressure drop through the normalized channel length*

Pressure drop increases with the size of wall roughness. As can be seen in Figure 9, the values of pressure drop reaches approximately to 1150 Pa for air and 1900 Pa for water, with an uptrend along the normalized channel length. The pressure drop that water experiences is significantly higher compared to air due to higher density and viscosity of water, which result in greater shear stress, hence greater resistance to flow. The increased pressure drop for water indicates a higher energy requirement for pumping the fluid through the channel, which is an important consideration.

In their smooth walled micro-channel with a D_h of 1mm, Quand Mudawar [6] reported a pressure drop ranging between 0.5 to 1.5 kPa.

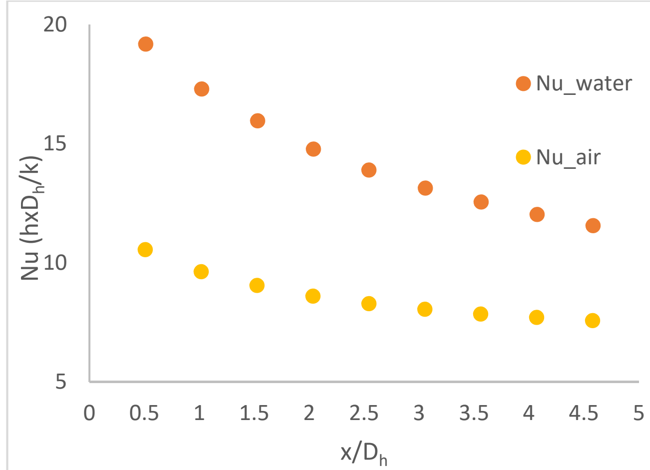

Figure 10. *Variation of Nusselt number through normalized channel length*

From Figures 9 and 10, it can be seen that the Nusselt number for both air and water show a slight decrease along the channel length that corresponds to the gradual increase in the development of flow, decreasing by 28% from about 10.54 to 7.56. While the Nusselt number for water is consistently higher than that for air, ranging from about 19.17 to 11.55, corresponding to a 65% decrease. In the upstream section, both water and air exhibit relatively high Nusselt numbers thanks to the strong convective heat transfer due to thin thermal boundary layer. As the fluid progresses downstream, the Nusselt number gradually decreases as a result of the grow in thermal boundary layer that induce a reduction in the overall heat transfer efficiency. The periodic corrugation along the sidewalls improves heat transfer by disrupting the boundary layer and enhancing local mixing. However, as the flow develops, the influence weakens and Nusselt number approaches to a stable figure.

Comparing the two fluids, water exhibits consistently higher Nusselt numbers than air, which is attributed to its superior thermal conductivity and Prandtl number. Despite this difference in magnitude, both fluids follow a similar trend in heat transfer behavior, suggesting that the enhancement mechanism due to corrugation affects them in a comparable manner. The steeper decline in the Nusselt number near the channel entrance implies that the flow is in the thermal entrance region, where boundary layer development is still in progress. As the normalized channel length increases, the boundary layer thickens, and the flow transitions toward a more thermally developed state, where the Nusselt number stabilizes.

As shown in Figure 11, the Nusselt number and pressure drop data obtained in a rectangular mini channel with corrugated side walls at different Reynolds numbers clearly demonstrate the effects of the flow regime and fluid properties on heat transfer and flow resistance.

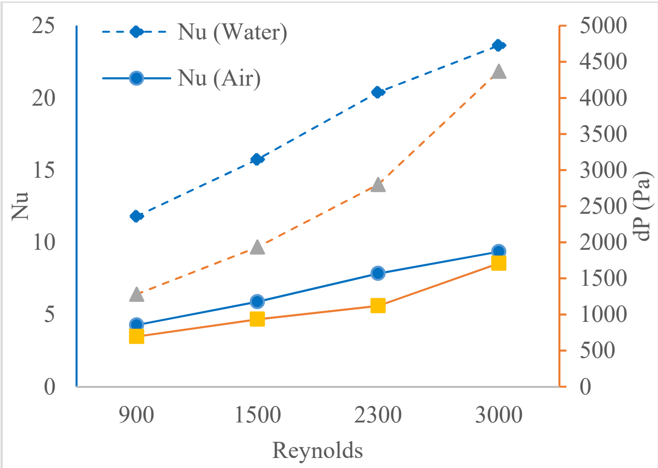

Figure 11. *Variation of Nusselt number through normalized channel length*

The results show that the Nusselt number for both water and air increase significantly with the increase in Reynolds number. This increase can be explained by the thinning of the thermal boundary layer and the strengthening of convective heat transfer due to the intense interaction of the fluid with the channel walls at higher flow rates. Water showed higher Nusselt numbers than air at all Reynolds numbers. This is related to the higher thermal conductivity and Prandtl number of water and shows that the heat transfer capacity of water is more effective than air. On the other hand, the pressure drop for both air and water increased significantly with the increase in Reynolds number. Water causes more pressure loss than air due to its low viscosity and high density. Especially at Re=3000, ΔP for water reaches approximately 4500 Pa, while this value remains around 1800 Pa for air. This situation causes the need for more pumping power in return for the high heat transfer advantage.

As a result, while the heat transfer enhancing effect of the corrugated sidewall structure becomes especially evident at low and medium Reynolds numbers, increased pressure losses at high Reynolds numbers can become a factor that can limit the overall efficiency of the system. Therefore, it is clear that in systems where such structures will be applied, pump costs should be taken into consideration in addition to the targeted cooling performance. In this context, the use of non-dimensional parameters such as performance evaluation criteria (PEC) can provide a balanced optimization of both the thermal and hydraulic efficiency of the system.

The results demonstrated that corrugated sidewalls in mini-channels can be an effective strategy for enhancing convective heat transfer while maintaining an acceptable pressure drop. These findings contribute to the design of high-performance heat sinks for electronic cooling applications, where compact and efficient heat dissipation is crucial.

To ensure the accuracy and reliability of the numerical simulations, the results were compared with experimental and numerical studies in the literature detailed in Table 2. The Nusselt number and pressure drop values were compared with the findings of Karabulut [52] and Sadighi Dizaji et al. [53].

Sadighi Dizaji et al. [53] experimentally investigated the tubes with corrugated surface profile in double pipe heat exchangers. They evaluated the inner and outer tubes as concave and convex separately (Figure 12) and reported that corrugated tubes provide significant increase in the performance of the heat exchanger compared to straight tubes. These results support the findings obtained in our study.

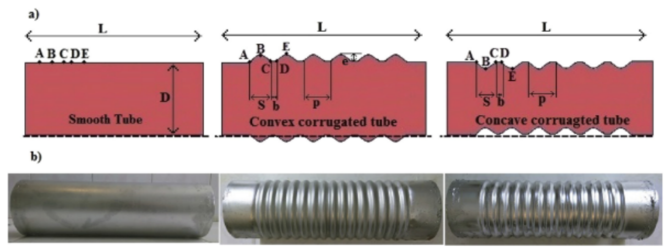

Figure 12. *Smooth and corrugated pipes used in a DPHE [53]*

Both studies examine the effects of surface geometry on heat transfer and flow properties. Both studies show that corrugated surfaces and surface roughness improve heat transfer by increasing flow mixing, but this also significantly increases pressure drop. In this context, both studies emphasize the need to strike a balance between increased heat transfer and pumping power requirements.

When various groove profiles are compared (Figure 13), it is seen that the cylindrical groove geometry maintains high thermal performance coefficients, especially at high Reynolds values.

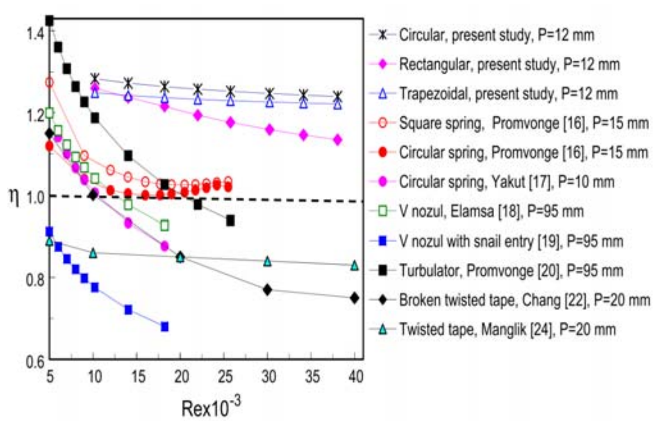

Figure 13. *Thermal performances of various grooved pipes and channels [54]*

Considering Bilen et al. [54] and our study, both investigate the effects of surface geometry on heat transfer and flow properties under turbulent flow conditions. Both studies emphasize the importance of optimizing the balance between heat transfer enhancement and energy losses and reveal the critical role of surface geometry on thermal performance.

Similarly, the results obtained by Sui et al. [55], who investigated the fluid flow in microchannels with different wave profiles, show that microchannels provide better heat transfer performance compared to straight channels.

a

b

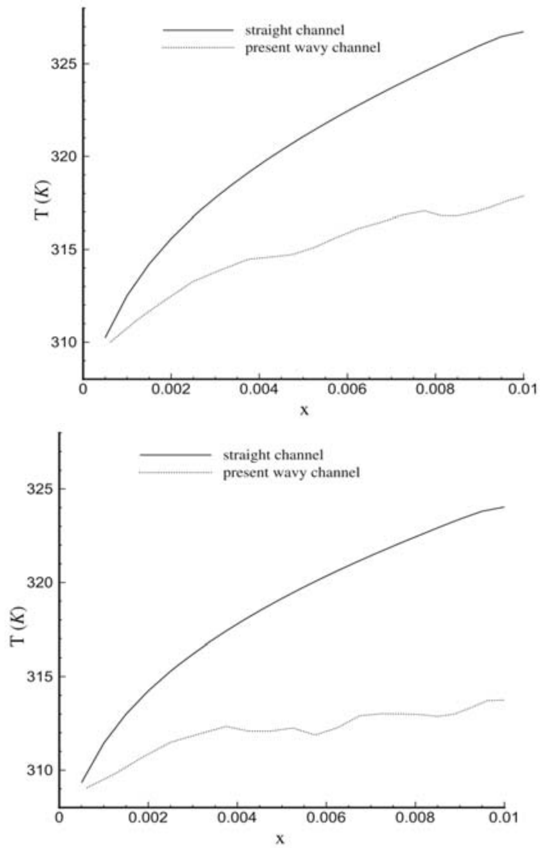

Figure 14. *Temperature distribution along the wavy micro channels (a) Re=300, (b) Re=400 [55]*

Sui et al. [55] and the present study, both of which investigated the effect of surface geometry on heat transfer and flow characteristics in small-scale mini channels, emphasize that optimized surface geometry is a critical design element to improve heat transfer while reducing energy losses. As can be seen in Figure 14, the temperature profile is very similar to what observed in the numerical simulation presented in Figure 14.

Harikrishnanand Tiwari [56] studied the fluid flow in the streamwise and spanwise corrugated channels for fixed channel width and height and compared them in terms of Nu and friction coefficients. The results showed that the turbulent kinetic energy occurs at higher values in the YZ plane in the transverse corrugated channel. (Figure 15).

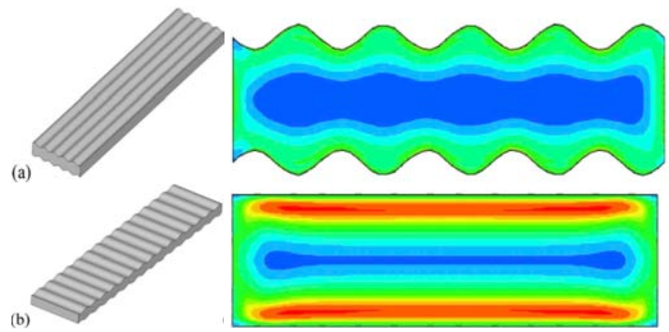

Figure 15. *Turbulent kinetic energy in the YZ-plane in fluid flow in (a) streamwise and (b) spanwise wavy channels [56]*

Harikrishnanand Tiwari [56] also investigated the effects of corrugated surface geometries on flow and heat transfer using numerical methods. Both studies pointed out that the surface geometry increases heat transfer by creating turbulence and secondary flows in the flow field, and emphasized that these geometric arrangements can increase energy efficiency with design optimization.

Begag et al. [57], who investigated the effects of corrugated surfaces on flow and heat transfer with numerical methods, as in the present study, analyzed the heat transfer and pressure drop performance of a channel with trapezoidal-shaped corrugations at different inclination angles under constant heat flux and for turbulent flow. In the present proposed study, the effects of corrugated surface profile and surface roughness on heat transfer and flow characteristics in a rectangular cross-section mini-channel were investigated. Both studies revealed that corrugated surfaces significantly improved heat transfer by increasing turbulence and mixing in the flow field, but this caused a higher pressure drop. It was also emphasized that the surface geometry increased heat transfer through the breaking and destabilization of the thermal boundary layer. These results indicate that the surface geometry should be carefully designed to increase energy efficiency and optimize pumping power requirements.

4. Conclusion

This numerical analysis investigated the impact of a corrugated surface profile on heat transfer and fluid flow characteristics in a turbulent flow through a rectangular mini-channel, considering both air and water as working fluids. The heat transfer characteristics in mini-channels are different from the experimental results of conventional sized channels. In experiments on flow and heat transfer in mini-channels, it is difficult to accurately measure some parameters such as channel dimensions, average roughness, local heat convection, local value of static pressure along the channel, etc. The study comprehensively examined velocity and temperature profiles, streamline patterns, pressure drop, and Nusselt number variations in order to provide a thorough understanding of the flow behavior of these fluids through the channel. By studying the surface roughness, it was observed that the important effect of this steady flow on local heat transfer can be understood.

The velocity and temperature profiles revealed that both air and water exhibit a high-velocity core with significant deceleration near the corrugated walls. Air showed a more abrupt velocity gradient and pronounced entrance and exit effects due to its lower density and viscosity. In contrast, water maintained a more uniform flow profile and absorbed heat more efficiently due to its higher density and specific heat capacity. Streamline analysis highlighted the formation of vortices and recirculation zones near the corrugated walls for both fluids, with water exhibiting more pronounced turbulence and mixing. These interactions suggest that the corrugated design effectively enhances turbulence and heat transfer, particularly for water. The evaluation of pressure drop and Nusselt number demonstrated that both parameters increase with the size of wall roughness. Water experienced significantly higher pressure drops compared to air, reflecting greater flow resistance due to its physical properties. However, water consistently achieved higher Nusselt numbers, indicating superior heat transfer performance.

In conclusion, the corrugated surface profile enhances heat transfer by promoting turbulence and mixing near the walls. While water provides better heat transfer performance, it also incurs higher pressure drops, necessitating a careful balance between thermal efficiency and energy consumption in practical applications. This study underscores the importance of fluid properties and surface design in optimizing the thermal performance of heat exchangers and similar systems, offering a foundation for future research and development in this field. As a suggestion for the future of this research, other changes in geometry and flow, such as fluid velocity and the height of the inlet and outlet openings of the channel, as well as the use advanced heat transfer fluids or nanofluids, can be used.

References

[1] Pettersen, J., 2004. Flow vaporization of CO2 in microchannel tubes, *Experimental thermal and fluid science*, *28*(2-3), pp.111–121.

[2] Siddique, W., El-Gabry, L., Shevchuk, I.V., Hushmandi, N.B., and Fransson, T.H., 2012. Flow structure, heat transfer and pressure drop in varying aspect ratio two-pass rectangular smooth channels, *Heat Mass Transfer*, *48*(5), pp.735–748.

[3] Kandlikar, S.G., and Upadhye, H.R., 2005. Extending the heat flux limit with enhanced microchannels in direct single-phase cooling of computer chips, *Semiconductor Thermal Measurement and Management IEEE Twenty First Annual IEEE Symposium*.

[4] Tuckerman, D.B., and Pease, R.F.W., 1981. High-performance heat sinking for VLSI, *IEEE Electron device letters*, *2*(5), pp.126–129.

[5] Kandlikar, S.G., 2005. Heat transfer mechanisms in microchannels and their engineering applications, *J. Heat Transfer*, *127*(1), pp.8–16.

[6] Qu, W., and Mudawar, I., 2002. Experimental and numerical study of pressure drop and heat transfer in a single-phase micro-channel heat sink, *International Journal of Heat and Mass Transfer*, *45*(12), pp.2549–2565.

[7] Kandlikar, S.G., and Grande, W.J., 2004. Evolution of microchannel flow passages–thermohydraulic performance and fabrication technology, *Heat Transfer Engineering*, *25*(3), pp.3–17.

[8] Lee, P.S., and Garimella, S.V., 2006. Thermally developing flow and heat transfer in rectangular microchannels of different aspect ratios, *International Journal of Heat and Mass Transfer*, *49*(17-18), pp.3060–3067.

[9] Harley, J., Bau, H., Zemel, J.N., and Dominko, V., 20-22 Feb. 1989. "Fluid flow in micron and submicron size channels", in: *IEEE Micro Electro Mechanical Systems, , Proceedings, 'An Investigation of Micro Structures, Sensors, Actuators, Machines and Robots',* IEEE, pp. 25–28.

[10] Peng, X.F., and Peterson, G.P., 1996. Convective heat transfer and flow friction for water flow in microchannel structures, *International Journal of Heat and Mass Transfer*, *39*(12), pp.2599–2608.

[11] Peng, X.-F., and Wang, B.-X., 1998. "Forced-convection and boiling characteristics in microchannels", in: *International Heat Transfer Conference Digital Library,* Begel House Inc.

[12] Shah, R.K., and London, A.L., 1978. "Rectangular Ducts", in: Shah, R.K., and London, A.L., eds., *Laminar flow forced convection in ducts,* Acad. Pr, New York, pp. 196–222.

[13] Steinke, M.E., and Kandlikar, S.G., 2006. Single-phase liquid friction factors in microchannels, *International Journal of Thermal Sciences*, *45*(11), pp.1073–1083.

[14] Wang, M., Zhang, W., Xin, G., Li, F., Pu, J.H., and Du, M., 2023. Improved thermal–hydraulic performance of a microchannel with hierarchical honeycomb porous ribs, *Can J Chem Eng*, *101*(2), pp.1083–1094.

[15] Flockhart, S.M., Dhariwal, R.S., 1998. Experimental and numerical investigation into the flow characteristics of channels etched in 〈100〉 silicon.

[16] Cisneros-Ramírez, C.-A., 2022. Review of the calculation of the boiling heat transfer coefficient in mini-channels and micro-channels, *TSE*, *4*(1), pp.1.

[17] Anwar, M., Tariq, H., Shoukat, A., Ali, H., and Ali, H., 2020. Numerical study for heat transfer enhancement

using CuO water nanofluids through mini-channel heat sinks for microprocessor cooling, *Therm sci*, *24*(5 Part A), pp.2965–2976.

[18] Kadivar, M., Tormey, D., and McGranaghan, G., 2022. CFD of roughness effects on laminar heat transfer applied to additive manufactured minichannels, *Heat Mass Transfer*.

[19] Lin, Y.-L., Shih, T.I.-P., Stephens, M.A., and Chyu, M.K., 2001. A Numerical Study of Flow and Heat Transfer in a Smooth and Ribbed U-Duct With and Without Rotation, *Journal of Heat Transfer*, *123*(2), pp.219–232.

[20] Akbarzadeh, M., Rashidi, S., Karimi, N., and Omar, N., 2019. First and second laws of thermodynamics analysis of nanofluid flow inside a heat exchanger duct with wavy walls and a porous insert, *J Therm Anal Calorim*, *135*(1), pp.177–194.

[21] Al-Hadhrami, L., Griffith, T., and Han, J.-C., 2003. Heat Transfer in Two-Pass Rotating Rectangular Channels (AR=2) With Five Different Orientations of 45 Deg V-Shaped Rib Turbulators, *Journal of Heat Transfer*, *125*(2), pp.232–242.

[22] Herman, C., and Kang, E., 2001. An Experimantal Study of Convective Heat Transfer Enhancement in a Grooved Channel Using Cylindrical Eddy Promoters, *JEH(T)*, *8*(6), pp.353–371.

[23] Alhamid, J., Al-Obaidi, A.R., and Towsyfyan, H., 2022. A numerical study to investigate the effect of turbulators on thermal flow and heat performance of a 3D pipe, *Heat Trans*, *51*(3), pp.2458–2475.

[24] Al-Obaidi, A.R., Alhamid, J., and Hamad, F., 2021. Flow felid and heat transfer enhancement investigations by using a combination of corrugated tubes with a twisted tape within 3D circular tube based on different dimple configurations, *Heat Trans*, *50*(7), pp.6868–6885.

[25] Mezaache, A., Louhichi, K., and Bessaïh, R., 2023. Numerical investigation of mixed convection and entropy production of nanofluid flow in a corrugated channel using a two-phase mixture model, *Heat Trans*, *52*(1), pp.734–758.

[26] Haj Maideen, R.B., and Somu, S., 2020. Design and analysis of double-pipe heat exchanger with new arrangements of corrugated tubes using honeycomb arrangements, *Thermal Science*, *24*(1 Part B), pp.635–643.

[27] Choudhary, P., and Ray, R.K., 2022. MHD natural convection in a corrugated enclosure with discrete isothermal heating, *Heat Trans*, *51*(6), pp.5919–5951.

[28] Sruthi, B., Sasidhar, A., Surendra Kumar, A., and Sahu, M.K., 2021. Comparative analysis of corrugation effect on thermohydraulic performance of double-pipe heat exchangers, *Heat Trans*, *50*(5), pp.4622–4642.

[29] Song, K.-W., and Wang, L.-B., 2013. The Effectiveness of Secondary Flow Produced by Vortex Generators Mounted on Both Surfaces of the Fin to Enhance Heat Transfer in a Flat Tube Bank Fin Heat Exchanger, *Journal of Heat Transfer*, *135*(4).

[30] Kandlikar, S.G., 2005. Characterization of surface roughness effects on pressure drop in single-phase flow in minichannels, *Physics of Fluids*, *17*(10).

[31] Badruddin, I.A., Ahmed N. J., S., Al-Rashed, A.A.A.A., Nik-Ghazali, N., Jameel, M., Kamangar, S., Khaleed, H.M.T., and Khan, T.M.Y., 2015. Conjugate Heat Transfer in an Annulus with Porous Medium Fixed Between Solids, *Transp Porous Med*, *109*(3), pp.589–608.

[32] Tao, W.-Q., 1987. Conjugated Laminar Forced Convective Heat Transfer From Internally Finned Tubes, *Journal of Heat Transfer*, *109*(3), pp.791–795.

[33] Morrison, F.A., 2001. *Understanding rheology,* Oxford University Press, New York, xiii, 545.

[34] Qin, S.-C., Zhang, Y.-C., Jiang, W., Zhang, X.-C., and Tu, S.-T., 2025. Structure optimization and design of zigzag mini-channel for printed circuit heat exchanger, *Applied Thermal Engineering*, *262,* pp.125207.

[35] Patankar, S.V., 1980. *Numerical Heat Transfer and Fluid Flow.tif,* Hemisphere Publishing Corporation, 200 p.

[36] Hinze, J.O., 1967. Secondary Currents in Wall Turbulence, *The Physics of Fluids*, *10*(9), S122-S125.

[37] Zeng, L., Pan, D., Ye, S., and Shao, X., 2019. A fast multiobjective optimization approach to S-duct scoop inlets design with both inflow and outflow, *Proceedings of the Institution of Mechanical Engineers, Part G: Journal of Aerospace Engineering*, *233*(9), pp.3381–3394.

[38] Chen, D., Müller-Eschner, M., Tengg-Kobligk, H. von, Barber, D., Böckler, D., Hose, R., and Ventikos, Y., 2013. A patient-specific study of type-B aortic dissection: evaluation of true-false lumen blood exchange, *Biomedical engineering online*, *12,* pp.65.

[39] Robinson, A., Eastwick, C., and Morvan, H., 2010. "Further Computational Investigations Into Aero-Engine Bearing Chamber Off-Take Flows", in: *ASME Turbo Expo 2010,* ASME, [Place of publication not identified], pp. 209–217.

[40] Bai, G., Armenante, P.M., Plank, R.V., Gentzler, M., Ford, K., and Harmon, P., 2007. Hydrodynamic

investigation of USP dissolution test apparatus II, *Journal of pharmaceutical sciences*, *96*(9), pp.2327–2349.

[41] Noui, Z., Si-Ameur, M., Bessanane, N., Djebara, A., Ibrahim, A., Ishak, M.A.A.B., Ajeel, R.K., and Dol, S.S., 2025. Comparative study of thermohydraulic performance in mini-channel heat sink systems: Multi-objective optimization and exergy considerations, *Case Studies in Thermal Engineering*, *66,* pp.105722.

[42] Karabulut, K., 2024. The effects of rectangular baffle angles and heights on heat transfer and pressure drop performance in cross-triangular grooved rectangular flow ducts, *International journal of heat and fluid flow*, *105,* pp.109260.

[43] Liang, S., Nie, J., Liu, J., Wang, Z., Li, Z., Hu, Z., Yuan, D., Zhang, J., and Feng, Z., 2025. Effect of longitudinal vortex induced by double square wire coils on the hydrothermal performance and entropy generation in the mini-channel heat sink, *Thermal Science and Engineering Progress*, *57,* pp.103162.

[44] Gnielinski, V., 1976. New Equations for Heat and Mass Transfer in Turbulent Pipe and Channel Flow, *International Chemical Engineering*, *16*(2), pp.359–367.

[45] Petukhov, B.S., 1970. Heat Transfer and Friction in Turbulent Pipe Flow with Variable Physical Properties, *Advances in Heat Transfer*, *6,* pp.503–564.

[46] Rhim, Y.C., and White, F.M., 2016. *Fluid mechanics,* McGraw-Hill education, New York, NY, 773 p.

[47] Alkhazaleh, A., Alnaimat, F., and Mathew, B., 2023. Fluid flow and heat transfer behavior of a liquid based MEMS heat sink having wavy microchannels integrating circular pin-fins, *International Journal of Thermofluids*, *20,* pp.100480.

[48] Liu, X., Zhang, H., Wang, F., Zhu, C., Li, Z., Zhao, D., Jiang, H., Liu, Y., and Zhang, Z., 2022. Thermal and hydraulic performances of the wavy microchannel heat sink with fan-shaped ribs on the sidewall, *International Journal of Thermal Sciences*, *179,* pp.107688.

[49] Li, W., Kadam, S., and Yu, Z., 2023. Heat transfer enhancement of tubes in various shapes potentially applied to CO2 heat exchangers in refrigeration systems: Review and assessment, *International Journal of Thermofluids*, *20,* pp.100511.

[50] Ji, W.-T., Fan, J.-F., Zhao, C.-Y., and Tao, W.-Q., 2019. A revised performance evaluation method for energy saving effectiveness of heat transfer enhancement techniques, *International Journal of Heat and Mass Transfer*, *138,* pp.1142–1153.

[51] Mohammed, H.A., Abed, A.M., and Wahid, M.A., 2013. The effects of geometrical parameters of a corrugated channel with in out-of-phase arrangement, *International Communications in Heat and Mass Transfer*, *40,* pp.47–57.

[52] Karabulut, K., 2020. Heat transfer and pressure drop evaluation of different triangular baffle placement angles in cross-corrugated triangular channels, *Therm sci*, *24*(1 Part A), pp.355–365.

[53] Sadighi Dizaji, H., Jafarmadar, S., and Mobadersani, F., 2015. Experimental studies on heat transfer and pressure drop characteristics for new arrangements of corrugated tubes in a double pipe heat exchanger, *International Journal of Thermal Sciences*, *96,* pp.211–220.

[54] Bilen, K., Cetin, M., Gul, H., and Balta, T., 2009. The investigation of groove geometry effect on heat transfer for internally grooved tubes, *Applied Thermal Engineering*, *29*(4), pp.753–761.

[55] Sui, Y., Teo, C.J., Lee, P.S., Chew, Y.T., and Shu, C., 2010. Fluid flow and heat transfer in wavy microchannels, *International Journal of Heat and Mass Transfer*, *53*(13-14), pp.2760–2772.

[56] Harikrishnan, S., and Tiwari, S., 2019. Heat transfer characteristics of sinusoidal wavy channel with secondary corrugations, *International Journal of Thermal Sciences*, *145,* pp.105973.

[57] Begag, A., Saim, R., Öztop, H.F., and Abboudi, S., 2021. Numerical Study on Heat Transfer and Pressure Drop in a Mini-Channel with Corrugated Walls, *Journal of Applied and Computational Mechanics*, *7*(3), pp.1306–1314.